

Spiral crystal growth

Peter Smereka *

Department of Mathematics, University of Michigan, Ann Arbor, MI 48109, USA

Received 22 March 1999; accepted 11 October 1999

Communicated by H. Müller-Krumbhaar

Abstract

We numerically study the spiral mode of crystal growth using a theory developed by Burton, Cabrera and Frank using a level set method. This method is novel in that it can handle not only closed curves but open curves as well. We use our method to compute interacting spirals and make estimates of growth rates. We also propose a possible coarsening mechanism for a large number of interacting spirals. ©2000 Elsevier Science B.V. All rights reserved.

Keywords: BCF theory; Crystal growth; Interacting spirals

1. Introduction

It is well documented that crystals grow in spiral patterns under a wide variety of growth conditions; see, e.g., the review article by Chernov [4]. This growth mechanism seems particularly important in the epitaxial growth of high-temperature superconducting thin films. In the case of YBCO films spiral growth has been reported by a number of investigators; e.g., Klemen and Scheel [8], Luo et al. [9], Raistrick and Hawley [12], Schlom et al. [13] or Yeadon et al. [17].

The spirals are generally believed to be a step that terminates at a screw dislocation. A screw dislocation is line defect in the crystal that results in the discontinuous change in the displacement. If the screw dislocation intersects the crystal surface the discontinuous change in the displacement yields a step on the crystal surface. The step then provides a preferred site for atoms to bond. As the atoms attach to the step, it then moves normal to itself. Since the step is immobile at the screw dislocation it then moves around the screw dislocation in a spiral form. The motion of the step is well studied and the basic ideas originate with the terrace–step–kink model of Burton, Cabrera and Frank [2], henceforth denoted BCF. When the steps are well separated and the attachment rate of atoms to the step is fast they show that the normal velocity of a step-line is given by

$$v_n = v_\infty(1 - \lambda\kappa), \quad (1)$$

where v_∞ is the speed of a straight step-line, λ is the critical radius, and κ is the curvature of step-line. By step-line we mean the location of the step, see Fig. 1.

* Tel.: +1-734-763-5742.

E-mail address: psmereka@math.lsa.umich.edu (P. Smereka).

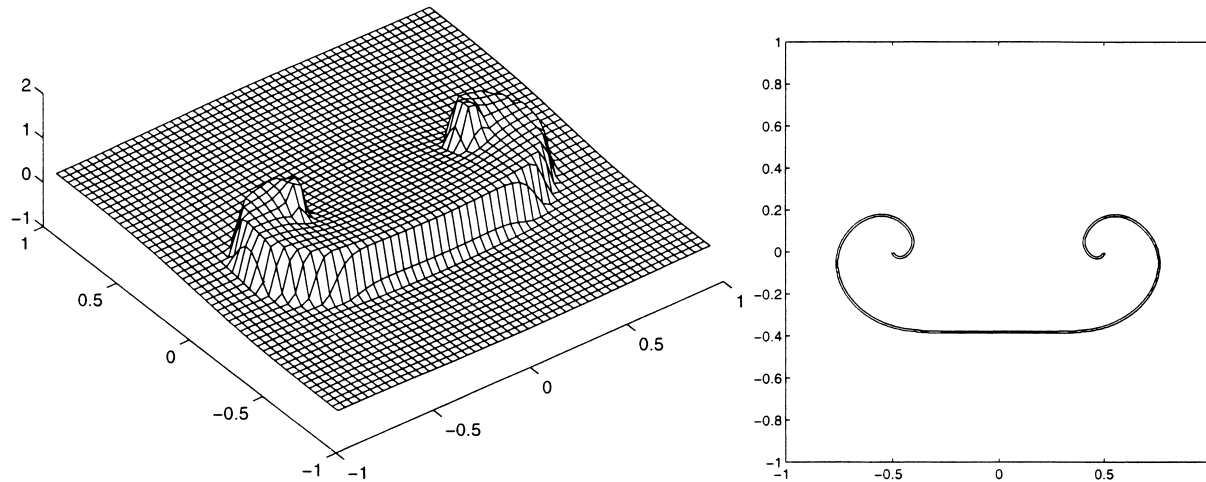


Fig. 1. The figure on the left shows the step between two screw dislocations while the figure on the right shows the step-line (which is an open curve).

If we start with a circular island of radius, R , then the island will grow if $R > \lambda$ and evaporate if $R < \lambda$. The authors develop an expression for v_∞ which depends on a number of physical parameters such as temperature and the surface diffusion coefficient. In this work we shall not concern ourselves with v_∞ and scale time and distance so that $v_\infty = 1$.

It should be pointed out that the assumption of well-separated steps means that the distance between steps is large compared to the distance an adatom diffuses before evaporating. This implies that for (1) to be a good approximation the desorption rate must be sufficiently large. If the desorption rate is not large enough the step velocity is not local and it is determined by solving a diffusion equation on the terraces. The effects of the desorption rate on the dynamics of spiral growth has recently been examined by Karma and Plapp [7] using a phase-field model. From their work one can infer the growth conditions for which (1) is a good approximation.

Let us consider the following situation: a step-line connecting two screw dislocations. Fig. 1 shows the step and the corresponding step-line. We will denote the step-line location by $\Gamma(t)$ which is given by

$$\Gamma(t) = \{\mathbf{x}(\alpha, t), \quad 0 \leq \alpha \leq 1\}.$$

The location of the two screw dislocations is $\mathbf{x}(0, t)$ and $\mathbf{x}(1, t)$. Since the screw dislocations do not move then $\mathbf{x}(0, t) = \mathbf{x}(0, 0)$ and $\mathbf{x}(1, t) = \mathbf{x}(1, 0)$.

The step-line is evolved using the BCF theory as follows:

$$\dot{\mathbf{x}}(\alpha, t) = (1 - \lambda\kappa)\mathbf{n}, \quad (2)$$

where \mathbf{n} is the unit normal to the step-line. The normal is given by

$$\mathbf{n} = \frac{1}{\sqrt{x_\alpha^2 + y_\alpha^2}} \begin{pmatrix} y_\alpha \\ -x_\alpha \end{pmatrix},$$

where x and y are the components of \mathbf{x} ($\mathbf{x} = (x, y)^T$) and the subscripts denote partial derivatives. The curvature is given by

$$\kappa = \frac{y_\alpha x_{\alpha\alpha} - x_\alpha y_{\alpha\alpha}}{(x_\alpha^2 + y_\alpha^2)^{3/2}}.$$

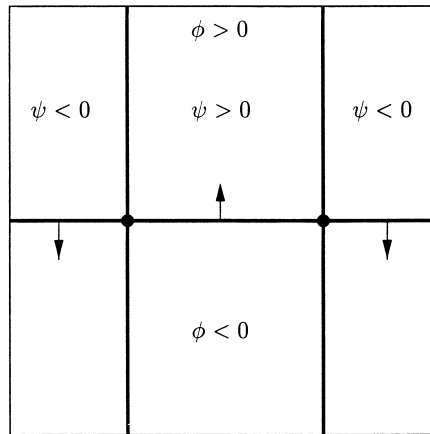


Fig. 2. The initial configuration — the screw dislocations are located by the two black dots and the physical step is the line connecting them. The horizontal line marks the set $\phi(\mathbf{x}, 0) = 0$. The two vertical lines mark the set $\psi(\mathbf{x}, 0) = 0$. The arrows mark the normals for the physical and artificial step-line as given by (6).

The dynamics of the spiral growth mode using (2) was examined in the BCF paper. They computed growth rates for single spirals and showed that (2) had a self-similar spiral solution. They also made several conjectures about interacting spirals. They considered two screw dislocations separated by a distance ℓ . When the spirals rotate in the opposite direction they argue that if $2/\lambda < \ell < 3/\lambda$ the growth of a pair of spirals will exceed the growth of single spiral by a few percent. If $\ell > 3/\lambda$ then the pair will have a growth rate exponentially close to that of a single spiral. When the spirals are co-rotating they conjecture that the growth rate will increase with decreasing separation and when the separation tends to zero the growth rate will be double that of a single spiral. The results obtained in this paper are in general agreement with these conjectures.

Cabrera and Levine [3] generalized (2) to include elastic effects. They also examined the self-similar solution in more detail. Schulze and Kohn [14] developed a geometric model to study the growth and interactions of many spirals. They used their model to predict, among other things, coarsening rates. We shall make some connections with this work in the last section of the paper.

There have been other theoretical investigations in the spiral motion of the step-lines which gave similar results to the BCF model. Müller-Krumbhaar et al. [10] derived a Ginzburg–Landau type equation which in a certain limit would reduce to the BCF model. Falo et al. [5] used a Langevin dynamical approach to calculate crystals growing in the spiral mode. Xiao et al. [18] used a Monte Carlo method to simulate the spiral growth mode. More recently, Aranson et al. [1] used a Ginzburg–Landau theory to the spiral growth model.

The goal of this paper is to study (2) by direct numerical computation. One possible approach to numerically compute the motion of the step-line would be to spatially discretize (2) and then solve the resulting system of ordinary differential equations. This Lagrangian approach has two difficulties. First, as the step-line evolves the points used to discretize the step-line may either spread out or bunch up. Thus one may need to either add more points or reparameterize the step-line so that the points are evenly spaced. The second difficulty is that the step-line may either self-intersect or merge with another step-line.

Although both difficulties can certainly be overcome we shall present a method based on a level set formulation which avoids both difficulties. In level set methods an interface is represented as the zero level set of a continuous function. The level set function is then evolved by solving a partial differential equation on a fixed grid. The location of the interface is then captured by plotting the contour of the zero level of the level set function. The advantage of such an approach is that topology changes are handled automatically. The method was first implemented numerically

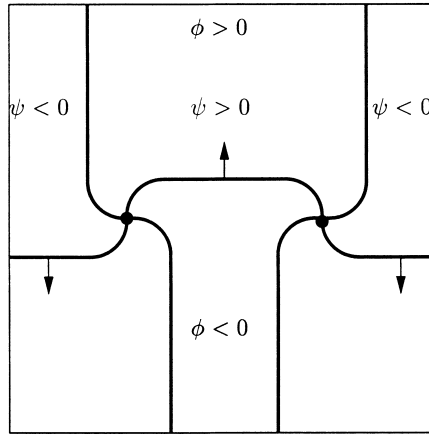


Fig. 3. Fig. 2 at slightly later time.

by Osher and Sethian [11] for fronts with curvature dependent speed. The method has since been used on a wide variety of problems. In this paper we shall present a modification of the level set method for the motion of step-lines. Such modification is necessary since there is no robust way to make an open curve a zero level set of a continuous function. Thus the level set method presented here is capable of computing both open and closed curves.

2. Level set approach

We shall denote our domain as Ω and take $\Omega = \{-L < x < L, -L < y < L\}$. Consider first the situation of the closed step-line (no screw dislocations) in Ω . We shall denote the initial location of the step-line as $\Gamma(0)$. Furthermore, we shall pick a continuous function, $\phi(\mathbf{x}, 0)$, defined on Ω so that its zero level set marks the location of the step-line; in other words

$$\Gamma(0) = \{\phi(\mathbf{x}, 0) = 0\}.$$

The unit normal to the interface and the curvature are then

$$\mathbf{n} = \frac{\nabla \phi}{|\nabla \phi|} \Big|_{\phi=0} \quad \text{and} \quad \kappa = \nabla \cdot \mathbf{n} \Big|_{\phi=0}.$$

Next, we define

$$\mathbf{v} = \left[1 - \lambda \nabla \cdot \left(\frac{\nabla \phi}{|\nabla \phi|} \right) \right] \frac{\nabla \phi}{|\nabla \phi|}.$$

We note that \mathbf{v} is defined everywhere on Ω and \mathbf{v} evaluated at $\phi = 0$ gives the BCF velocity. ϕ is then updated with the following transport equation:

$$\frac{\partial \phi}{\partial t} + \mathbf{v} \cdot \nabla \phi = 0, \tag{3}$$

with boundary conditions

$$\frac{\partial \phi}{\partial n} = 0, \quad \mathbf{x} \in \partial \Omega. \tag{4}$$

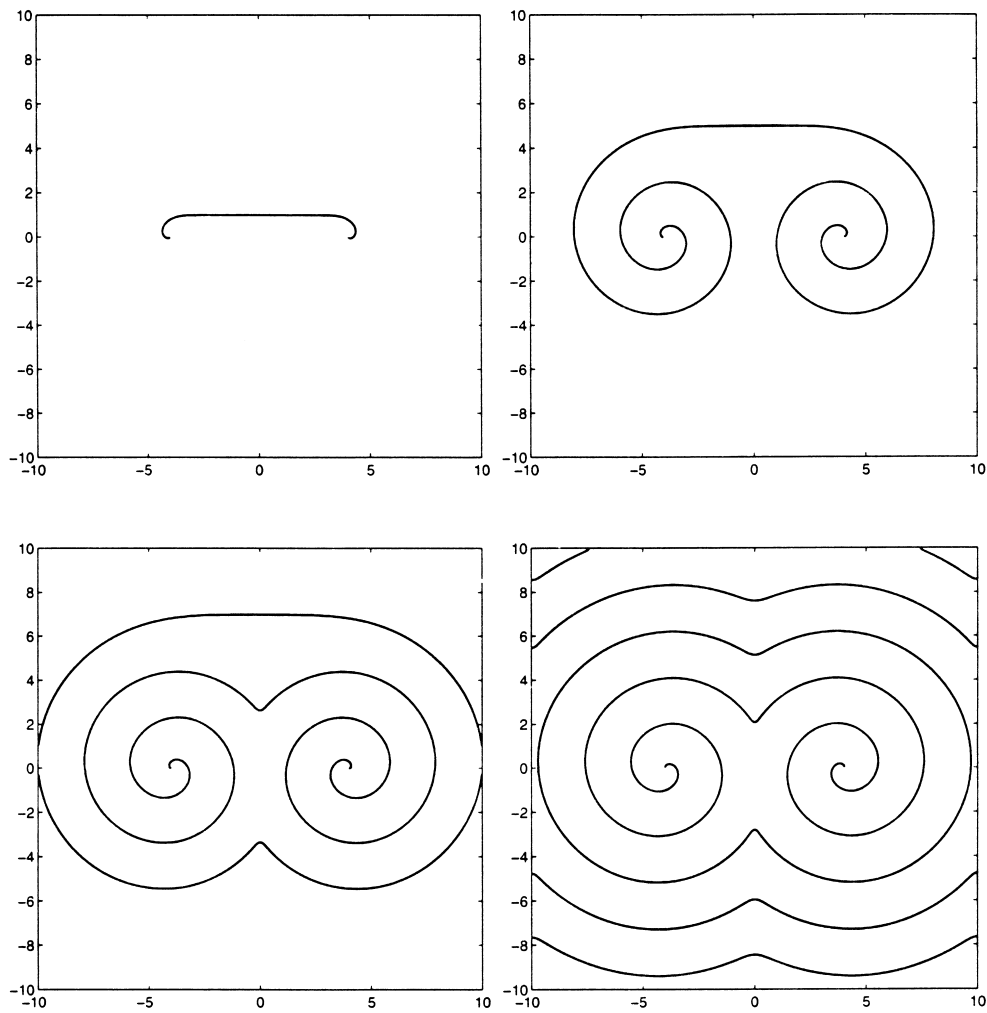


Fig. 4. The motion of the step-line is shown at various times with initial conditions given by Eq. (19) with $\lambda = 0.1$. The times shown are $t = 1, 5, 7$ and 11 (from left to right and top to bottom).

The location of the step-line is then given by the zero level set of ϕ , i.e.

$$\Gamma(t) = \{\phi(\mathbf{x}, t) = 0\}.$$

Let us now consider a modification of the above method in order to include screw dislocations. This will be done using another level set function, ψ . In the following example we have a step between two screw dislocations. The initial location of the step-line is given by

$$\Gamma(0) = \{\phi(\mathbf{x}, 0) = 0, \psi(\mathbf{x}, 0) > 0\}.$$

We note that the screw dislocations are located where $\phi = 0$ and $\psi = 0$ and that the set $\phi = 0$ contains the physical step-line (where $\psi > 0$) and an artificial step-line (where $\psi < 0$). Our goal is to evolve both ϕ and ψ in such a way that

$$\Gamma(t) = \{\phi(\mathbf{x}, t) = 0, \psi(\mathbf{x}, t) > 0\}. \quad (5)$$

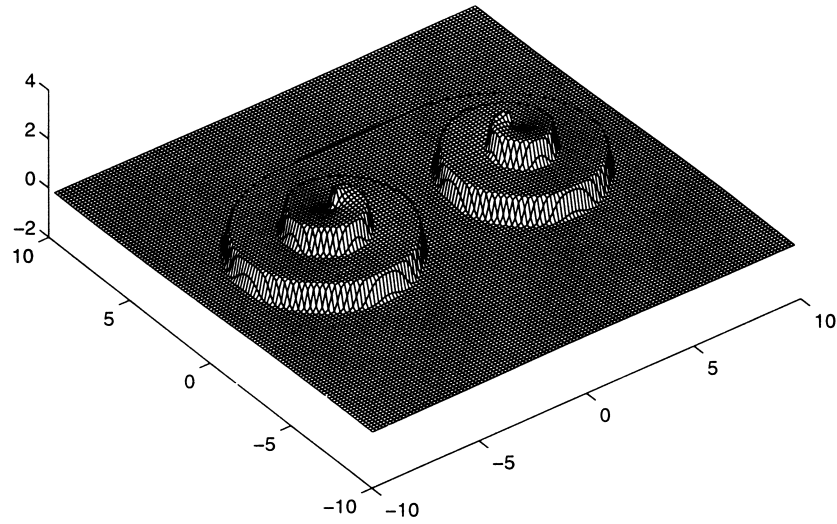


Fig. 5. This shows the height profile for the corresponding step-line shown in Fig. 4 at $t = 5$.

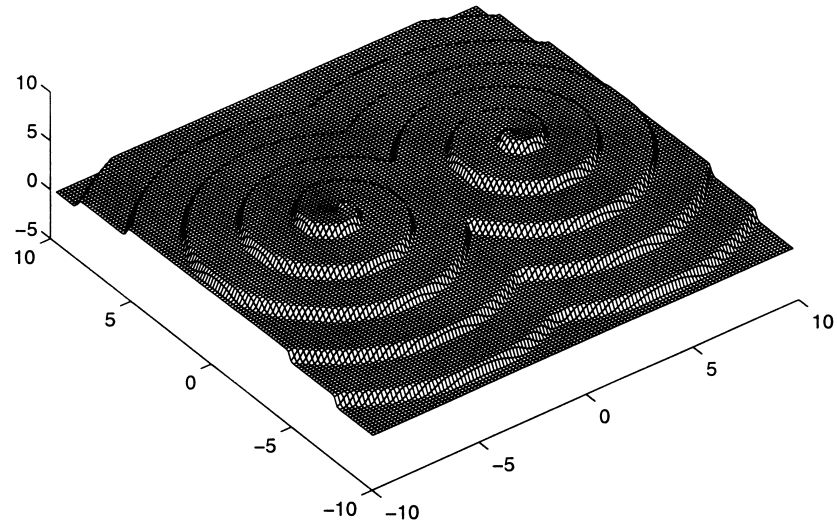


Fig. 6. This shows the height profile for the corresponding step-line shown in Fig. 4 at $t = 11$.

To achieve this goal we define the normal and the curvature of the step-line as

$$\mathbf{n} = \text{sgn}(\psi) \frac{\nabla \phi}{|\nabla \phi|} \quad (6)$$

and

$$\kappa = \text{sgn}(\psi) \mathcal{K}(\phi), \quad (7)$$

where

$$\mathcal{K}(\phi) = \nabla \cdot \left(\frac{\nabla \phi}{|\nabla \phi|} \right)$$

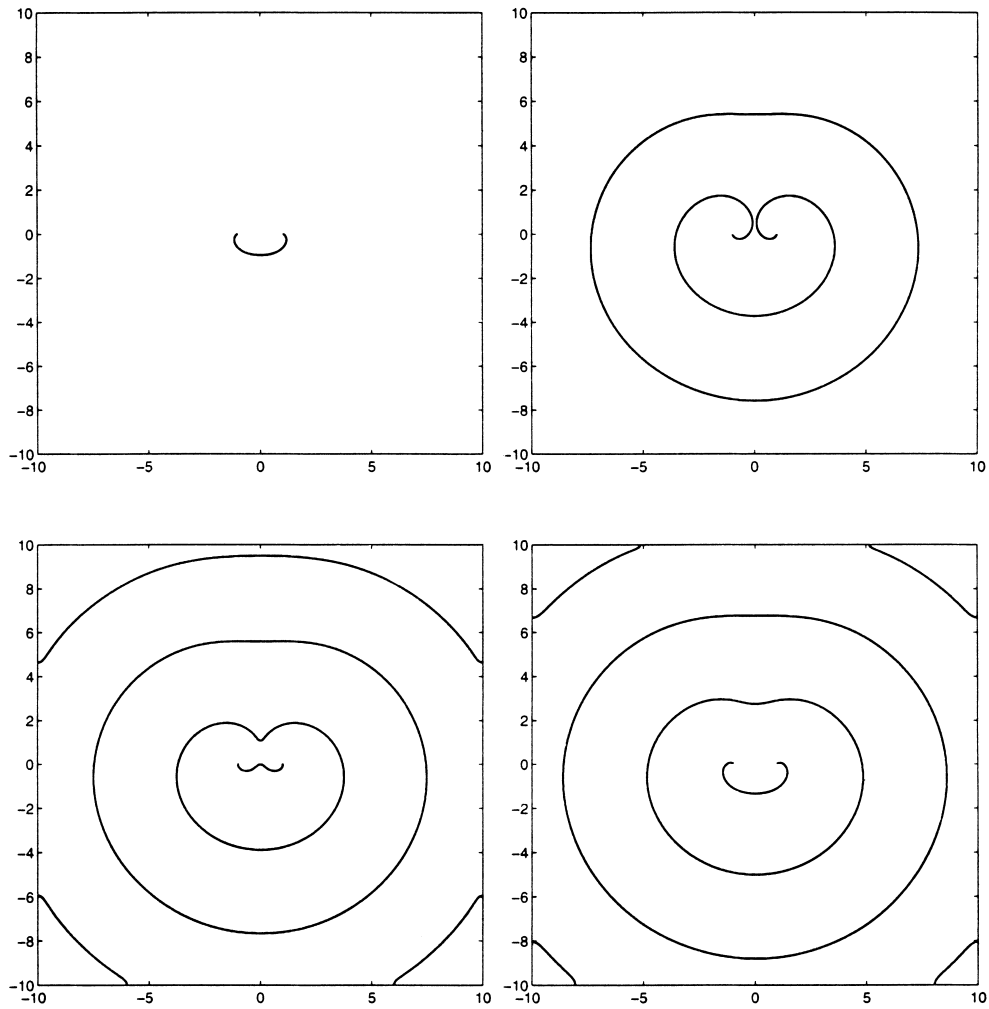


Fig. 7. The motion of the step-line is shown at various times for the oppositely rotating spirals. The initial conditions are given by Eq. (20) with $a = 1$, and λ is taken to be 0.2. The times shown are $t = 1, 8, 16$ and 25 (from left to right and top to bottom).

and

$$\text{sgn}(\phi) = \begin{cases} 1, & \phi > 1, \\ 0, & \phi = 0, \\ -1, & \phi < 0. \end{cases}$$

The key point here is that normal and the curvature change sign as one crosses $\psi = 0$ (as one moves from the physical step to the artificial step).

Next, we define the velocity field

$$\mathbf{v} = \text{sgn}(\psi) \frac{\nabla \phi}{|\nabla \phi|} (1 - \lambda \text{sgn}(\psi) \mathcal{K}(\phi)) \quad (8)$$

which means that the artificial step moves in the opposite direction to the actual step. Furthermore since $\text{sgn}(0) = 0$,

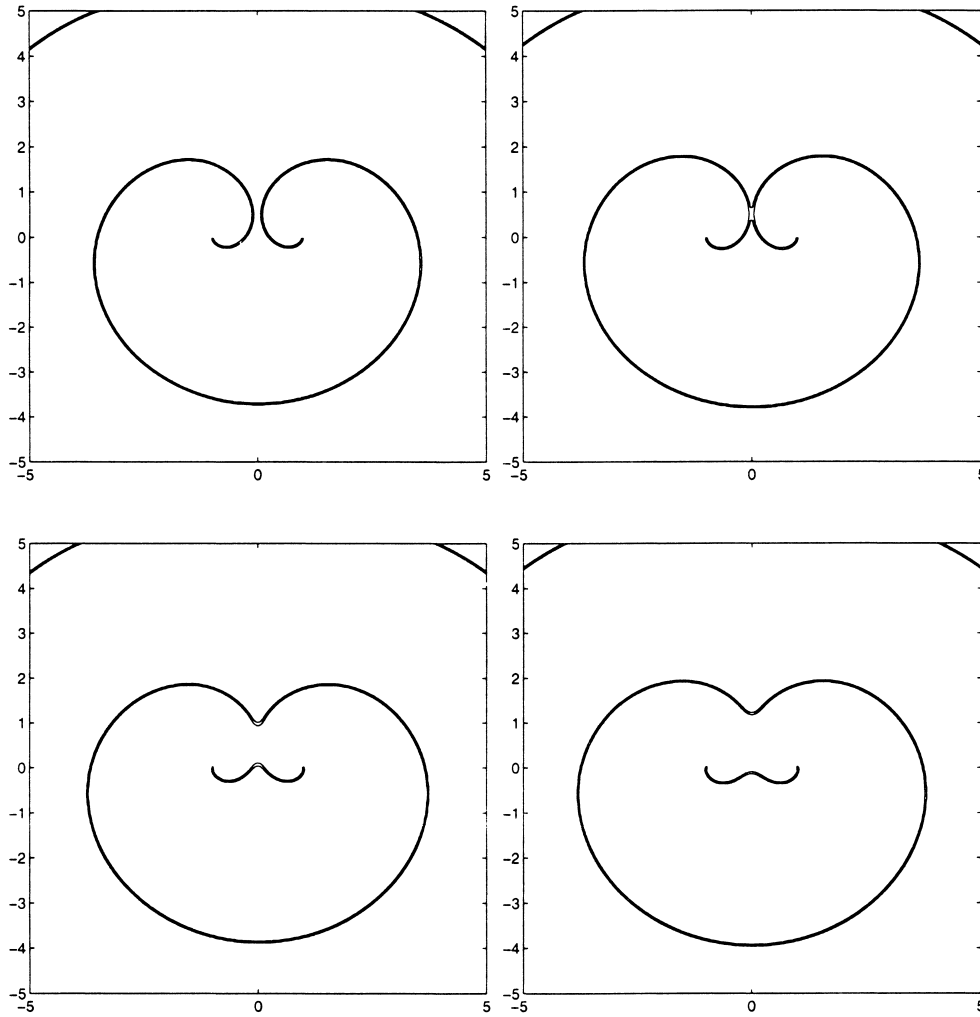


Fig. 8. The motion of the step-line is shown in more detail at various times for the oppositely rotating spirals. The conditions are the same as those in Fig. 7. The times shown are $t = 8, 8.08, 8.16$ and 8.24 (from left to right and top to bottom).

then the normal velocity of the step-line at the screw dislocations will be zero. If we substitute (8) into (3) we obtain

$$\frac{\partial \phi}{\partial t} + \text{sgn}(\psi)[1 - \lambda \text{sgn}(\psi)\mathcal{K}(\phi)]|\nabla \phi| = 0. \quad (9)$$

Ultimately this formulation will breakdown unless we also update ψ . This is done with the following “dual” equation:

$$\frac{\partial \psi}{\partial t} + \text{sgn}(\phi)[1 - \lambda \text{sgn}(\phi)\mathcal{K}(\psi)]|\nabla \psi| = 0. \quad (10)$$

When (9) and (10) are solved as a system the location of the step will be given by (5) (see Figs. 2 and 3).

Remark. *If we start with an initially straight step-line then at $t = 0$ the normal velocity of the physical step is 1 and for artificial step it is -1 except at the screw dislocation where both are zero. This means at $t = 0^+$ both step-lines will become curved at the screw dislocation.*

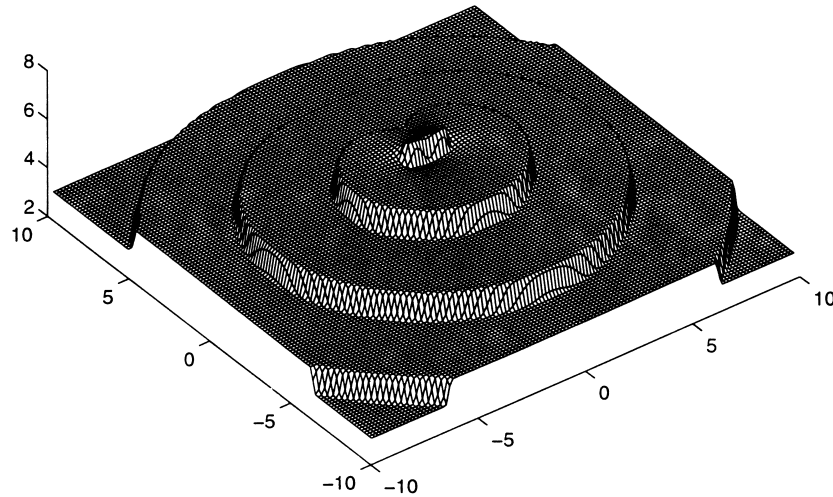


Fig. 9. The film height is shown at $t = 24$ for the oppositely rotating spirals. Parameters are the same as those in Fig. 7.

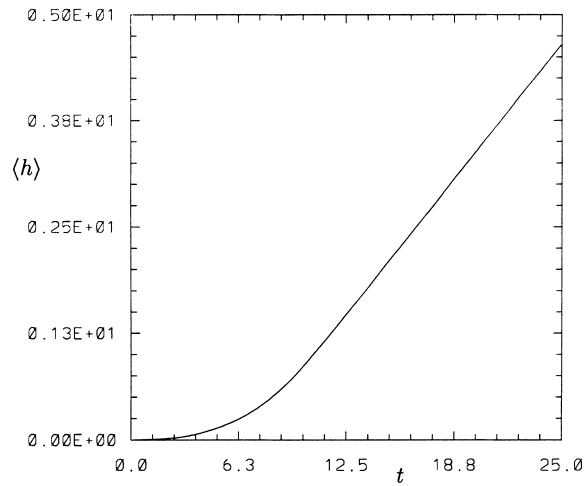


Fig. 10. The average height as a function of time is shown for the oppositely rotating spirals. Parameters are the same as those in Fig. 7.

We can also represent the step-line in a slightly different way; we define

$$\theta = \begin{cases} |\phi|, & \psi \geq 0, \\ 1, & \psi < 0, \end{cases} \quad (11)$$

thus

$$\Gamma(t) = \{\theta(\mathbf{x}, t) = 0\}.$$

2.1. Film height

The vertical displacement of the interface can be determined once the location of the step-line is known. We shall assume that the displacements are small and linear elasticity provides a good approximation. We will also

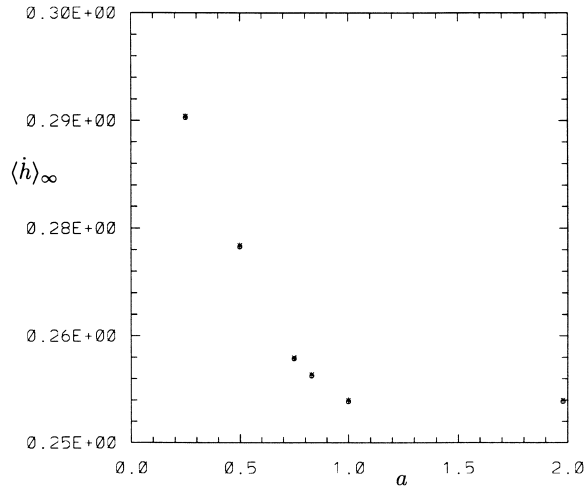


Fig. 11. Summarizes the asymptotic growth rates, $\langle \dot{h} \rangle_\infty$, as a function of a for the oppositely rotating spirals.

assume that the displacements in the x and y planes are zero, meaning that we have only displacement in the vertical direction. We let h denote the vertical displacement which is henceforth called the height. It then follows from basic linear elasticity that $\nabla^2 h = 0$, provided we are not on the step-line (see [6], p. 43). Furthermore we shall assume that the material is isotropic and that the screw dislocation is straight and perpendicular to the crystal surface. We take the Burger's vector to be $\mathbf{b} = b\mathbf{e}_z$; consequently at the step-line the height must jump by b . Given this, the height must satisfy

$$\nabla^2 h = -b\nabla \cdot (\delta_\Gamma \mathbf{n}) \quad (12)$$

with boundary conditions

$$\frac{\partial h}{\partial n} = 0, \quad \mathbf{x} \in \partial\Omega, \quad (13)$$

where δ_Γ is a delta function concentrated on the step-line. In terms of the level set functions (12) is written as

$$\nabla^2 h = -b\nabla \cdot (\delta(\phi)H(\psi)\nabla\phi), \quad (14)$$

where $H(x)$ is the Heaviside function. We remark that if the step-line is defined by $y = 0, x > 0$, then the solution of (12) is

$$h(x, y) = \frac{b}{2\pi} \tan^{-1} \frac{y}{x}$$

(see, e.g., [6], p. 59).

We must make sure Eq. (12) has a solution. It is easy to check that the solvability condition for (12) with (13) is

$$\int_{\Omega} \nabla \cdot (\delta_\Gamma \mathbf{n}) \, d\mathbf{x} = \int_{\partial\Omega} \delta_\Gamma \mathbf{n} \cdot \mathbf{n}_\Omega \, ds = 0, \quad (15)$$

where \mathbf{n}_Ω is a unit normal to the boundary of Ω . If the step-line does not cross the boundary of Ω then the above integral is zero since $\delta_\Gamma = 0$ for $\mathbf{x} \in \partial\Omega$. On the other hand if the step-line does cross the boundary then the integral is still zero because the boundary condition (4) ensures that $\mathbf{n} \cdot \mathbf{n}_\Omega = 0$. Therefore, we see that (12) with boundary conditions given by (13) has a solution.

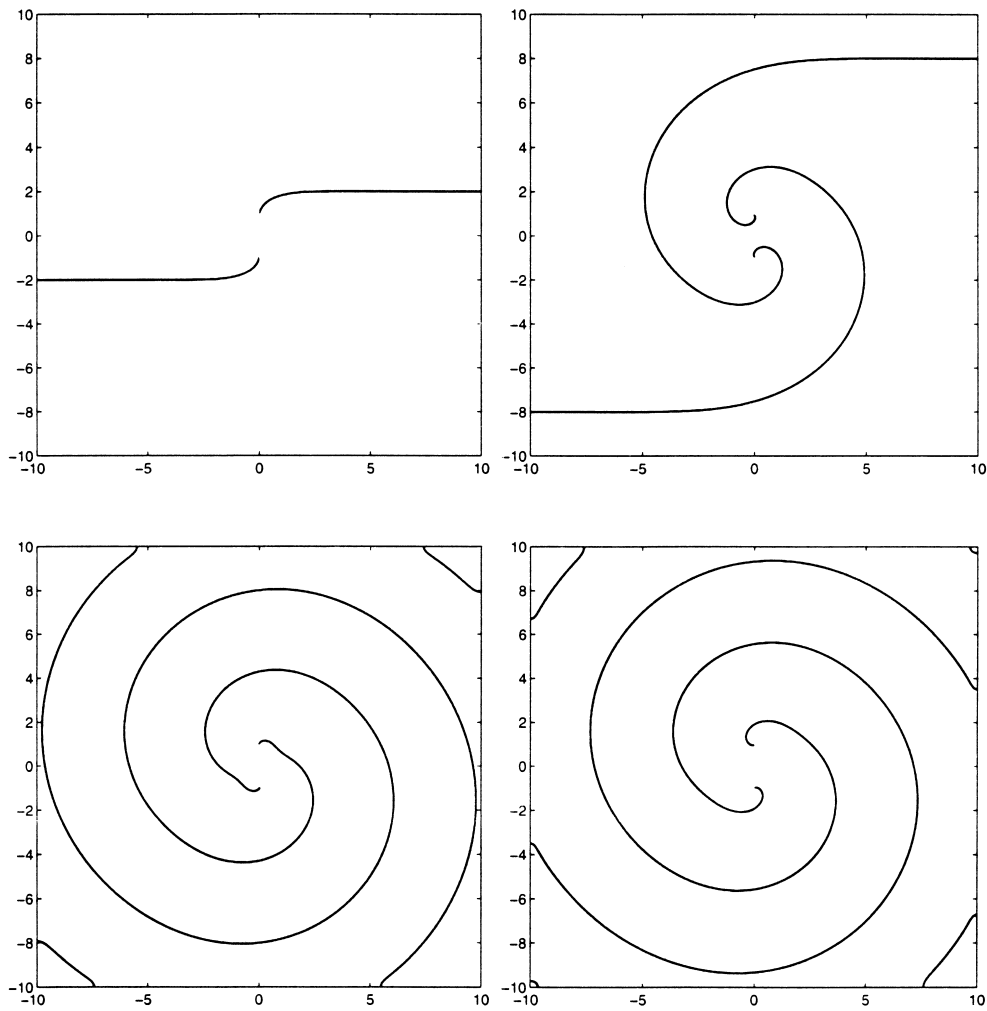


Fig. 12. The motion of the step-line is shown at various times for the co-rotating spirals. The initial conditions are given by Eq. (21) with $a = 1$, and λ is taken to be 0.2. The times shown are $t = 1, 7, 16$ and 25 (from left to right and top to bottom).

This solution is not unique since we may add a constant to it. This indicates that the average height must be determined from a separate calculation. Let us assume that the average height is initially zero and let $V(t)$ denote the volume of matter deposited on the film. Then the average height, $\langle h \rangle$, is

$$\langle h \rangle = \frac{V(t)}{A},$$

where $A = 4L^2$ is the area of the film. The rate of change of V is easily found to be

$$\dot{V} = b \int_{\Gamma} \mathbf{v} \cdot \mathbf{n} \, ds = b \int \mathbf{v} \cdot \mathbf{n} H(\psi) \delta(\phi) |\nabla \phi| \, d\mathbf{x}.$$

We solve (12) with the constraint that $\langle h \rangle = 0$ and then add $V(t)/A$ to h .

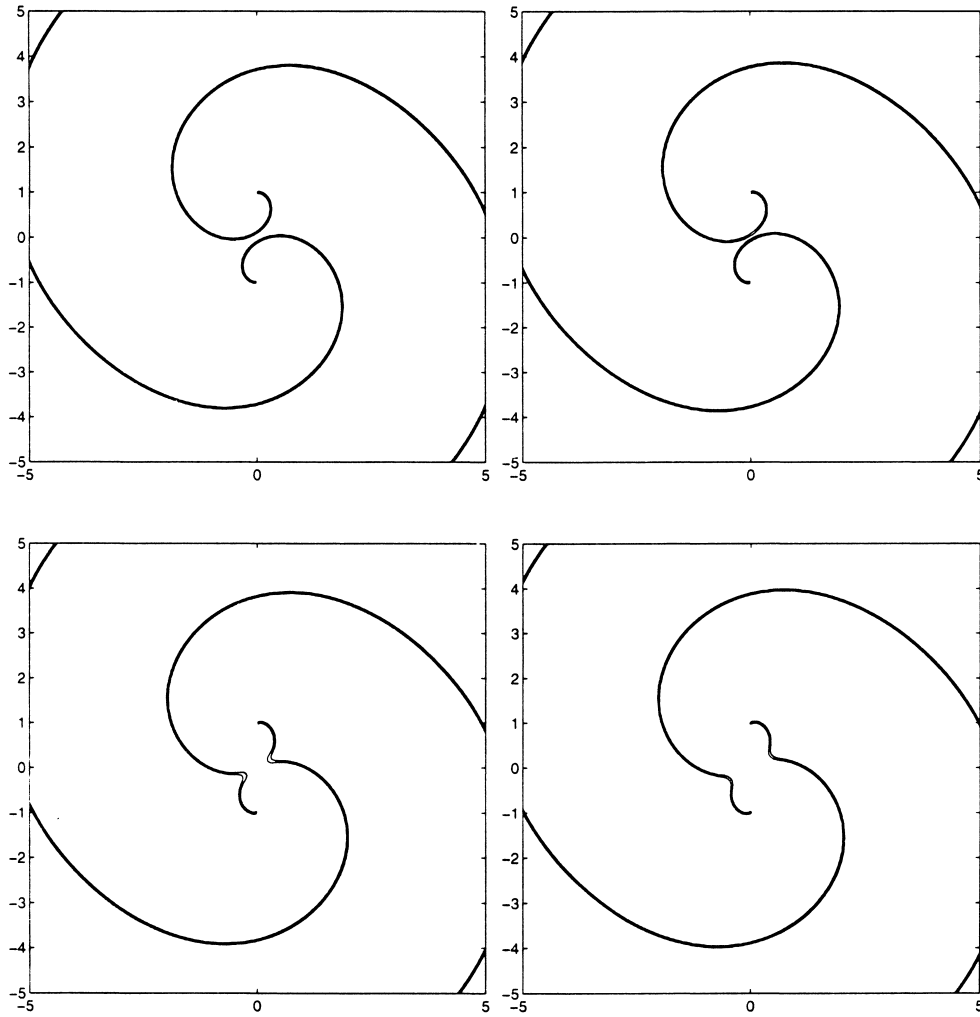


Fig. 13. The motion of the step-line is shown in more detail at various times for the co-rotating spirals. The conditions are the same as those in Fig. 12. The times shown are $t = 15.39, 15.45, 15.51$ and 15.57 (from left to right and top to bottom).

2.2. Numerical implementation

The numerical methods used to solve the relevant equations are standard and therefore we only briefly mention the numerical aspects of the work. To solve (9) and (10) numerically we first replace sgn by sgn_ε in both equations where sgn_ε is a mollification of sgn . In our computations we use

$$\text{sgn}_\varepsilon(\phi) = \begin{cases} 1, & \phi > \varepsilon, \\ \frac{\phi}{\varepsilon}, & |\phi| \leq \varepsilon, \\ -1, & \phi < -\varepsilon. \end{cases} \quad (16)$$

Eqs. (9) and (10) are then solved using first order upwind methods for the advection part and center differences for the curvature part. This is explained in [11,15].

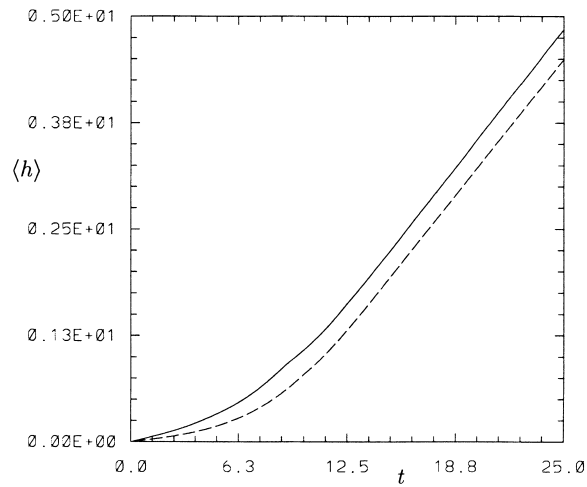


Fig. 14. The solid line shows the average height as a function of time for the co-rotating spirals and the dashed line shows the average height for a single spiral.

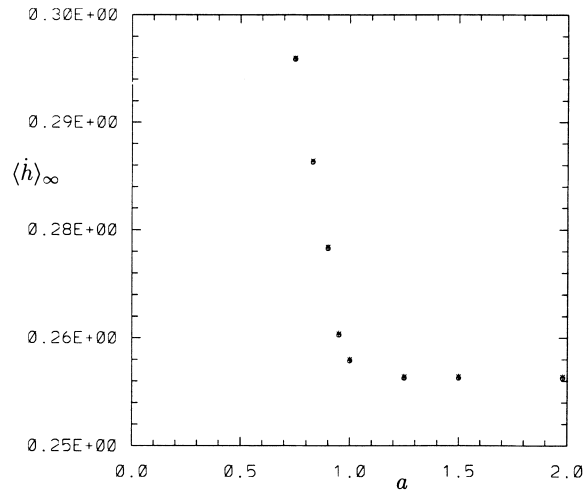


Fig. 15. Summarizes the asymptotic growth rates for various values of a for the co-rotating spirals. $\langle \dot{h} \rangle_{\infty}$ for a single spiral is approximately 0.253.

The delta function and the Heaviside function found in (14) are also replaced by mollified versions. We use

$$\delta_{\varepsilon}(\phi) = \begin{cases} 0, & |\phi| > \varepsilon, \\ \frac{1 + \cos(\pi \phi / \varepsilon)}{2\varepsilon}, & |\phi| \leq \varepsilon. \end{cases} \quad (17)$$

and

$$H_{\varepsilon}(\phi) = \begin{cases} 1, & \phi > \varepsilon, \\ \frac{\phi + \varepsilon}{2\varepsilon}, & |\phi| \leq \varepsilon, \\ 0, & \phi < -\varepsilon. \end{cases} \quad (18)$$

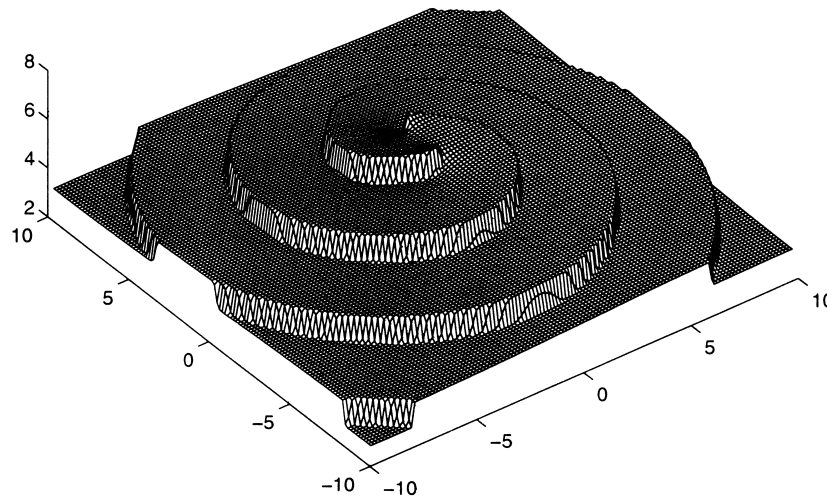


Fig. 16. The height profile at $t = 24$ for the co-rotating spiral case. The parameters are the same as those in Fig. 12.

Eq. (14) was then center differenced, the resulting linear system was then solved by a standard conjugate gradient algorithm. In the numerical computations that follow we take $\varepsilon = 4\Delta x$, where Δx is the size of the grid. It was found that the results were not very sensitive to the value of ε . We did find, however, that method converged faster for larger values of ε .

In our computations we constantly re-parameterize the level set functions ϕ and ψ so that $|\nabla\phi| = 1$ and $|\nabla\psi| = 1$. This is done using the method developed by Sussman et al. [16]. To plot the location of the interface we plot the zero contours of $\theta(\mathbf{x}, t) - \frac{1}{2}\Delta x$. This gives two lines on either side of the step-line (the lines are very close and when plotted they often look like a single line).

3. Results

For all of the computations presented in this section $\Omega = \{-10 < x < 10, -10 < y < 10\}$. Convergence studies were performed and we found that 500 grid points in each direction was sufficient to ensure a convergent answer. The time step, Δt , was chosen so that $\Delta t = 0.8\frac{1}{4}\lambda(\Delta x)^2$ which ensures that the numerical method will be stable.

3.1. Oppositely rotating spirals

In the first computation we consider two screw dislocations located at $(x, y) = (\pm 4, 0)$, the step-line connects these screw dislocations by a straight line. The step-line near the screw dislocation at $(4, 0)$ will rotate clockwise whereas the near $(-4, 0)$ the step-line will rotate counter-clockwise. To apply our level set method to simulate the dynamics of this step-line we initialize ϕ and ψ as follows:

$$\phi(\mathbf{x}, 0) = y \quad \text{and} \quad \psi(\mathbf{x}, 0) = 4 - |x|. \quad (19)$$

The results of the computations are shown in Figs. 4–6 where we have used $\lambda = 0.1$. Fig. 4 shows the location of the step-line at various times. We notice that up until $t = 5$ the step-line is an open curve but at $t \approx 6$ the step-line self-intersects and is now composed of an open curve joining the two screw dislocations and closed curves. This figure is very similar to a figure sketched in the BCF paper (see their Fig. 4).

Fig. 5 shows the height profile at $t = 5$ (before any step-line intersection has occurred). Here one sees two spiral towers. Fig. 6 shows the height profile $t = 11$ with two spiral towers resting on top of a series of terraces.

In the series of computations that follows we further examine the dynamics of a step-line connected to two screw dislocations located at $(x, y) = (\pm a, 0)$. The behavior of the step-lines as the distance between the screw dislocations, $2a$, is varied will be examined with $\lambda = 0.2$. We initialize ϕ and ψ as follows:

$$\phi(\mathbf{x}, 0) = y \quad \text{and} \quad \psi(\mathbf{x}, 0) = a - |x|. \quad (20)$$

The motion of step-line for $a = 1$ is shown at various times in Fig. 7. These figures show the step-line self-intersecting thus nucleating an island. The results shown in this figure are similar to scanned probe microscopy images of YBCO deposits on MgO obtained by Yeaton et al. [17]. Figs. 8 and 9 shows the height profile at $t = 24$.

Fig. 10 shows the average height as a function of time. It is evident from this figure that after $t \approx 12$ the slope of this graph is approximately constant. We shall call this the asymptotic growth rate, $\langle \dot{h} \rangle_\infty$. Fig. 11 presents the results of a series of computations where the asymptotic growth rate is computed for various values of a . The results show that as one reduces a the growth rate increases. One also notices that there appears to be a critical value of a , a^* and for $a > a^*$ the growth rate is the same as for the single spiral. This is because as one reduces a the spirals will touch before they can complete one rotation. Once they touch a region of large negative curvature forms and the effective rotation speed increases. Thus the time needed to nucleate a new island is reduced. Ultimately this will break down, as one reduces a below λ growth must stop.

The BCF paper has crude estimates of how the growth rate will depend on a . They find that if $\lambda < a < 1.5\lambda$ the growth rate will be a few percent larger than for a single spiral and if $a > 1.5\lambda$ then the difference from the single spiral will be exponentially small. Our numerical results are consistent with these predictions.

3.2. Co-rotating spirals

Next we consider the situation with two screw dislocation located at $(x, y) = (0, \pm a)$ with step-lines running off to infinity parallel to the x -axis. In this case the dislocations have the same sign and the step-lines will both rotate counter-clockwise. In the level set formulation of this situation we use the initial conditions

$$\phi(\mathbf{x}, 0) = -\min(y + a, -y + a) \quad \text{and} \quad \psi(\mathbf{x}, 0) = \min\left(2a + a\frac{x - L}{L}, y - a\frac{L - x}{L}\right), \quad (21)$$

where $L = 10$.

The motion of the step-lines is shown in Fig. 12. The step-lines move counter-clockwise around the screw dislocations and will, after a short time, intersect at which time the step-lines switch screw dislocations. This is closely related to the situation displayed in Figs. 5 and 6 of the BCF paper. The average height as function of time is shown in Figs. 13 and 14 also shown is the average height for a single spiral (the computations for the single spiral are included below). This figure shows that initially the growth rate for the co-rotating spirals is twice that of a single spiral as expected. It also shows that as time proceeds the single spiral appears to catch up. This is due to the fact that when the co-rotating spirals intersect they exchange centers and tend to unwind (see Fig. 13). This slows down their effective rotation rate and thus reduces the growth rate. Ultimately, the asymptotic growth rate for the co-rotating spirals is slightly greater than the single spiral. The asymptotic growth rate as a function of a is plotted in Fig. 15. These results show that the asymptotic growth rate for the co-rotating spirals is greater than that for a single spiral (which is 0.253). The results also demonstrate that the growth rate will increase as the distance between the screw dislocations is decreased, confirming arguments in the BCF paper. Fig. 15 also shows that for a approximately greater than 1 the growth rate will be the same as for the single spiral. The reason for this is that

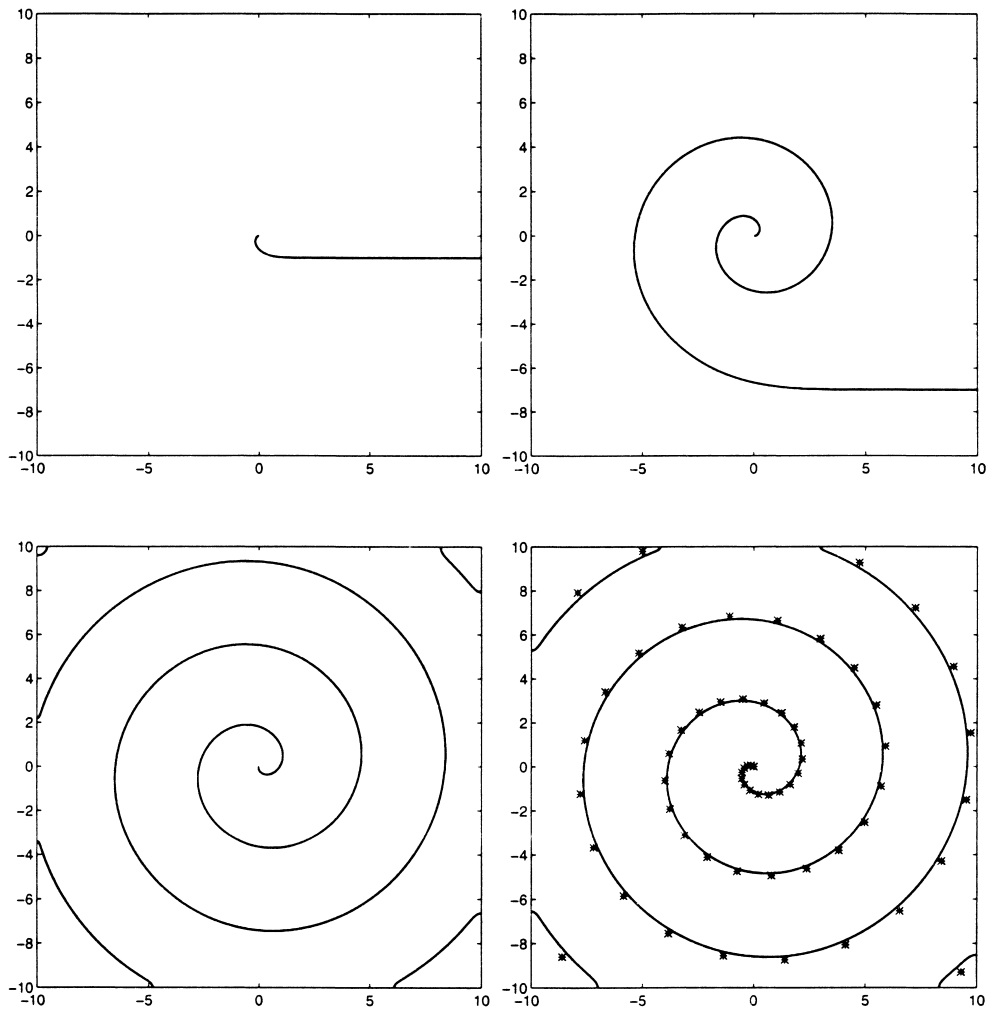


Fig. 17. The motion of the step-line is shown for a single spiral at various times with initial conditions given by Eq. (22) and $\lambda = 0.2$. The times shown are $t = 1, 7, 16$ and 25 (from left to right and top to bottom). In the last frame the spiral defined by Eq. (23) is plotted with asterisks.

when a is sufficiently large the spirals will be able to rotate once before interacting. Fig. 16 shows the height profile for the co-rotating spirals.

3.3. Single spiral

As a point of comparison we present the computation for a single step-line with a single screw dislocation. The single spiral is initialized with

$$\phi(\mathbf{x}, 0) = y \quad \text{and} \quad \psi(\mathbf{x}, 0) = x. \quad (22)$$

The motion of the step-line is shown in Fig. 17 and the height profile is shown in Fig. 18. It appears from Fig. 17 that by $t = 16$ the spiral is in steady rotation. The BCF paper gives an approximate expression for the shape of

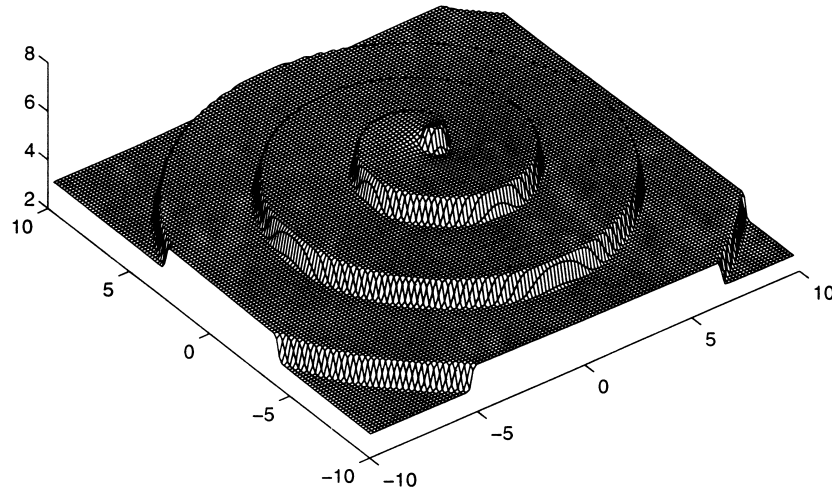


Fig. 18. The height profile for the single spiral case. The parameters are the same as those for Fig. 17.

steadily rotating spiral (see their Eq. (42)). In polar coordinates, their result is

$$\theta = \frac{\sqrt{3}}{2(1 + \sqrt{3})} \left[\frac{r}{\lambda} + \log \left(1 + \frac{r}{\lambda\sqrt{3}} \right) \right]. \quad (23)$$

In the last frame of Fig. 17 we present both the result of the level set computation and Eq. (23) and find good agreement.

Remark. In both Figs. 11 and 15 it appears that $\langle \dot{h} \rangle_\infty$ tends to value different than the value for a single spiral as a gets large. We attribute this difference to the fact that the computations are done in a domain with finite size.

3.4. Scaling

We can deduce the asymptotic growth rate for different values of λ from the results above by scaling. If we consider $L \rightarrow \infty$ then

$$\langle \dot{h} \rangle_\infty = \langle \dot{h} \rangle_\infty(a, \lambda).$$

Furthermore we can remove the dependence on λ in (2) by scaling \mathbf{x} and time by λ . This means, e.g., that the distance between the spiral arms scales with λ . It also follows that $\langle \dot{h} \rangle_\infty$ for different values of λ are related as follows:

$$\langle \dot{h} \rangle_\infty(a, \lambda) = \frac{\lambda_1}{\lambda} \langle \dot{h} \rangle_\infty \left(\frac{\lambda}{\lambda_1} a, \lambda_1 \right). \quad (24)$$

One can then use (24) and the numerical results for $\lambda = 0.2$ to find $\langle \dot{h} \rangle_\infty$ for different values of λ .

3.5. Coarsening

The motion of two step-lines each connecting two screw dislocations is considered in this section. According to our results from the previous section the smaller the distance between the screw dislocations, the faster the

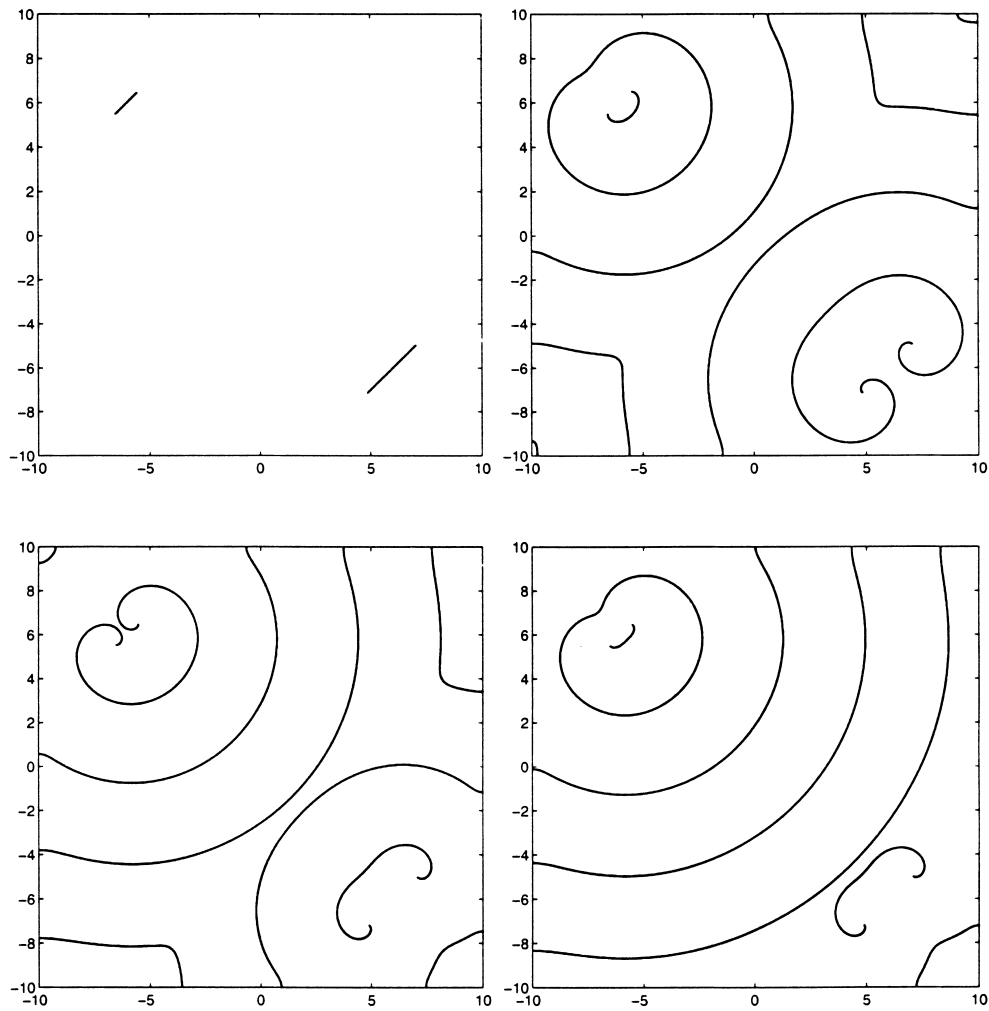


Fig. 19. The motion of two interacting step-lines is shown at various times with $\lambda = 0.2$. The initial conditions are given by Eq. (25). The distance between the screw dislocations is 1.44 (upper left corner) and 3.12 (lower right corner). The times shown are $t = 0, 16, 132$ and 358 (from left to right and top to bottom).

growth rate. This would indicate that step-lines associated with a smaller distance between the screw dislocations would overtake step-lines associated with a greater distance between the screw dislocations; thus step-lines with the smallest distance between screw dislocations would predominate. Therefore, it follows that a variability in the distance between screw dislocations provides a coarsening mechanism. This is illustrated in the following computation with the initial conditions:

$$\phi(\mathbf{x}, 0) = \min(x - y + 12, -x + y + 12) \quad \text{and} \quad \psi(\mathbf{x}, 0) = \min(x + 0.9y + 1, -x - 1.1y + 1). \quad (25)$$

These initial conditions give rise to two step-lines with lengths of 1.44 ($a = 0.72$) and 3.12 ($a = 1.56$) separated a distance of 16.97. The shorter one is in the upper left corner whereas the longer one in the lower right corner. According to the results summarized in Fig. 11 the spirals in the upper left corner will grow faster than the spirals in the lower right corner. Ultimately the spirals originating in the top left corner should slowly occupy a greater

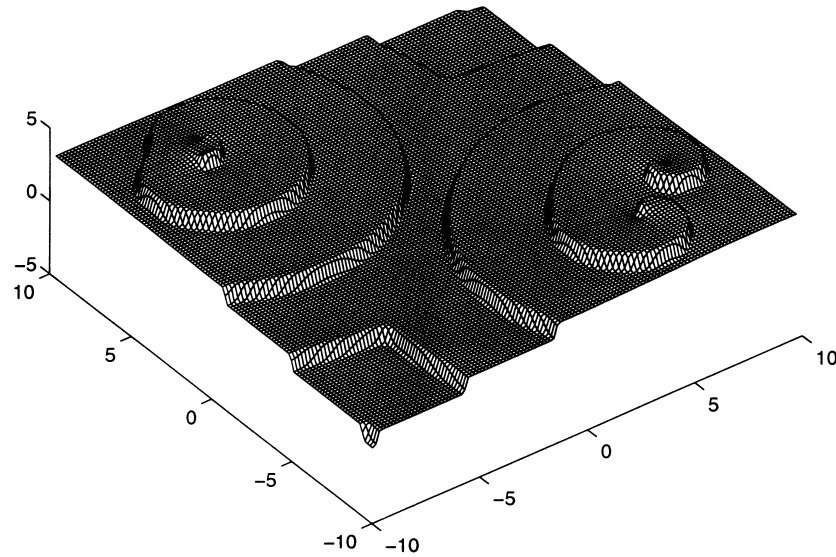


Fig. 20. The height profile for the interacting spiral case at $t = 16$. The parameters are the same as those in Fig. 19.

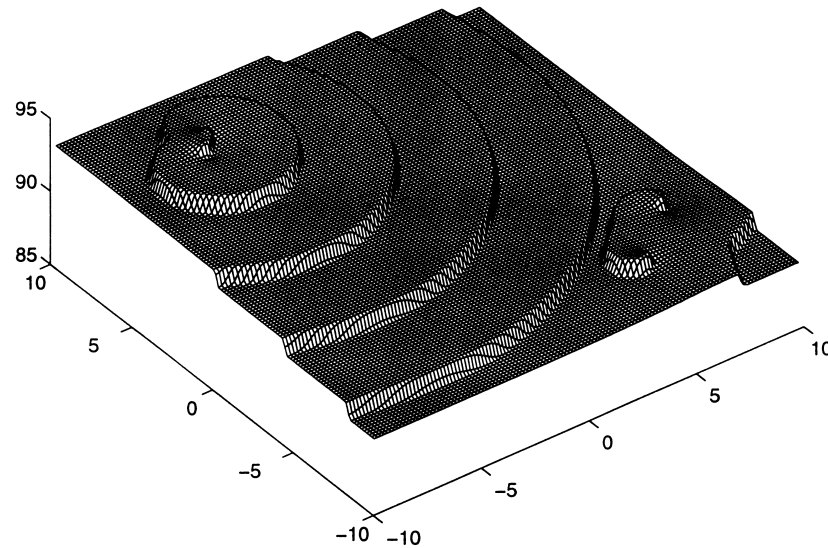


Fig. 21. The height profile for the interacting spiral case at $t = 358$. The parameters are the same as those in Fig. 19.

fraction of the substrate. The numerical results shown in Fig. 19 verify this claim. The film height is shown at two different times in Figs. 20 and 21.

In the above example we have considered the situation where the initial conditions consist of two step-lines. It is natural to ask: what the coarsening rate would be when the initial conditions contain a large number of step-lines. To answer this question it is useful to assume that the step-lines are far apart compared to the terrace widths. In this case the height function for a single pair of spirals is well approximated by a cone whose center is determined by the initial location of the step-line. The rate at which the cone grows is determined by the distance between the

screw dislocations. Thus the height profile may be approximated by a large number of cones growing at different rates.

This is the situation studied by Schulze and Kohn [14] in a different context. They considered a large number of interacting single spirals which were also approximated as cones with different growth rates. They then used their model to deduce statistical properties such as the coarsening rate and surface roughness in terms of the probability distribution of the growth rates. Therefore, one can combine their theory with the results in Fig. 11 to find statistical properties in terms of the probability distribution of the distance between screw dislocations.

Acknowledgements

The author thanks Brenda Brown for reading over this manuscript and also thanks Weinan E, Robert Kohn, and Tim Schulze for helpful discussions. This part was supported in part by NSF and DARPA through the Virtual Integrated Prototyping (VIP) initiative. This work was also supported in part by NSF through a Mathematical Sciences Career grant (Grant No. DMS-9625190).

References

- [1] I.S. Aranson, A.R. Bishop, I. Daruka, V.M. Vinohur, Ginzburg–Landau theory of spiral surface growth, *Phys. Rev. Lett.* 80 (1998) 1770–1773.
- [2] W.K. Burton, N. Cabrera, F.C. Frank, The growth of crystals and the equilibrium structure of their surfaces, *Phil. Trans. Roy. Soc. Lond.* 243A (1951) 299–358.
- [3] N. Cabrera, M.M. Levine, On the dislocation theory of evaporation of crystals, *Phil. Mag.* 1 (1956) 450–458.
- [4] A.A. Chernov, Formation of crystals in solutions, *Contemp. Phys.* 30 (1989) 251–276.
- [5] F. Falo, A.R. Bishop, P.S. Lomdahl, B. Horovitz, Langevin molecular dynamics of interfaces: nucleation versus spiral growth, *Phys. Rev. B* 43 (1991) 8081–8088.
- [6] J.P. Hirth, J. Lothe, *Theory of Dislocations*, McGraw-Hill, New York, 1968.
- [7] A. Karma, M. Plapp, Spiral surface growth without desorption, *Phys. Rev. Lett.* 81 (1998) 4444–4447.
- [8] C. Klemenz, H.J. Scheel, Flat $\text{YBa}_2\text{Cu}_3\text{O}_{7-x}$ layers for planar tunnel-device technology, *Physica C* 265 (1996) 126–134.
- [9] L. Luo, M.E. Hawley, C.J. Maggiore, R.C. Dye, R.E. Muenchausen, L. Chen, B. Schmidt, A.E. Kaloyeros, Spiral growth in epitaxial $\text{YBa}_2\text{Cu}_3\text{O}_{7-x}$ thin films produced by high deposition rate chemical vapor deposition, *Appl. Phys. Lett.* 62 (1993) 485–486.
- [10] H. Müller-Krumbhaar, T.W. Burkhardt, D.M. Kroll, Generalized kinetic equation for crystal growth, *J. Cryst. Growth* 38 (1977) 13–22.
- [11] S. Osher, J.A. Sethian, Fronts propagating with curvature-dependent speed, *J. Comp. Phys.* 79 (1988) 12–49.
- [12] I.D. Raistrick, M. Hawley, Scanning tunneling and atomic force microscopes studies of thin sputtered films of $\text{YBa}_2\text{Cu}_3\text{O}_{7-\delta}$, in: S.L. Shindé, D.A. Rudman (Eds.), *Interfaces in High- T_c Superconducting Systems*, Springer, New York, 1994, pp. 28–70.
- [13] D.G. Schlom, D. Anselmetti, J.G. Bednorz, J. Mannhart, Epitaxial growth of cuprate superconductors from the gas phase, *J. Cryst. Growth* 137 (1994) 259–267.
- [14] T.P. Schulze, R.V. Kohn, A geometric model for coarsening during spiral-mode growth of thin films, *Physica D* 132 (1999) 520–542.
- [15] J.A. Sethian, *Level Set Methods*, Cambridge University Press, New York, 1996.
- [16] M. Sussman, P. Smereka, S. Osher, A level set approach for computing the solutions to incompressible two-phase flow, *J. Comp. Phys.* 114 (1994) 146–159.
- [17] M. Yeadon, M. Aindow, F. Wellhöfer, J.S. Abell, Topographic development and misfit relief in laser-ablated heteroepitaxial $\text{YBa}_2\text{Cu}_3\text{O}_{7-\delta}$ thin films, *J. Cryst. Growth* 172 (1997) 145–155.
- [18] R. Xiao, J.I.D. Alexander, F. Rosenberger, Growth morphologies of crystal surfaces, *Phys. Rev. A* 43 (1991) 2976–2992.